

# Metastable decomposition of high-dimensional meteorological data with gaps

ILLIA HORENKO\*

INSTITUTE OF MATHEMATICS, FREE UNIVERSITY OF BERLIN, BERLIN, GERMANY

STAMEN I. DOLAPTCHIEV

POTSDAM INSTITUTE FOR CLIMATE IMPACT RESEARCH (PIK), POTSDAM, GERMANY

ALEXEY ELISEEV

A.M. OBUKHOV INSTITUTE OF ATMOSPHERIC PHYSICS (RAS), MOSCOW, RUSSIA

IGOR MOKHOV

A.M. OBUKHOV INSTITUTE OF ATMOSPHERIC PHYSICS (RAS), MOSCOW, RUSSIA

RUPERT KLEIN

INSTITUTE OF MATHEMATICS, FREE UNIVERSITY OF BERLIN, BERLIN, GERMANY

---

\*Corresponding author address: Illia Horenko, Institute of Mathematics, Free University of Berlin, Arn-

## ABSTRACT

We present an extension of the recently developed method for simultaneous dimension reduction and metastability analysis of high dimensional time series (see Horenko, to be published in The Journal of Atmospheric Sciences). The modified approach is based on a combination of ensembles of hidden Markov models (HMMs) with state-specific principal component analysis (PCA) in extended space (guaranteeing the overall dynamics to be Markovian). The main advantage of the modified method is its ability to deal with the gaps in the high-dimensional observation data. The proposed method allows (i) to separate the data according to the metastable states (ii) to perform a hierarchical decomposition of these sets into metastable substates, and (iii) to calculate the state-specific extended empirical orthogonal functions simultaneously with identification of the underlying Markovian dynamics switching between those metastable substates. We discuss the model assumptions introduced and explain how the quality of the resulting reduced representation can be assessed. We show what kind of additional insight into the underlying dynamics such a reduced Markovian representation can give, f. e., in the form of transition probabilities, statistical weights, mean first exit times and mean first passage times. We demonstrate the performance of the new method analyzing 500 hPa geopotential height fields (daily mean values from the ERA 40 data set for a period of 44 winters), compare the results with information gained from a numerically expensive but assumptions-free method ("Wavelets-

---

imallee 2-6, 14195 Berlin, Germany.

E-mail:horenko@math.fu-berlin.de

PCA”), and interpret the identified metastable states w.r.t. the blocking events in the atmosphere.

# Introduction

Many meteorological and climatological applications are characterized by the need to find some low-dimensional mathematical models for complex systems that undergo transitions between different phases. Such phases can be different circulation regimes in meteorology (Tsonis and Elsner 1990; Kimoto and Ghil 1993a,b; Cheng and Wallace 1993; Efimov et al. 1995; Mokhov and Semenov 1997; Mokhov et al. 1998; Corti et al. 1999; Palmer 1999) or glacial/interglacial sequences in climatology (Benzi et al. 1982; Nicolis 1982; Paillard 1998). Starting from the seminal paper by Charney and DeVore (Charney and Devore 1979), atmospheric blocking formation is also often associated with flip-flops between two states of atmospheric flow, one with strong (non-blocked) and other with blocked zonal flow. Regimes of this kind can sometimes be not directly observable (or "hidden") in many dimensions of the system's degrees of freedom and can exhibit persistent or metastable behavior (Majda et al. 2006; Franzke et al. 2007). If knowledge about the system is present only in the form of observation or measurement data, the challenging problem of identification of those metastable states together with construction of reduced low-dimensional models becomes a problem of time series analysis and pattern recognition in many dimensions. The choice of the appropriate data analysis strategies (implying a set of method-specific assumptions on the analyzed data) plays a crucial role in correct interpretation of the available time series.

In their recent pioneering works A. Majda and co-workers have demonstrated the presence of hidden persistent patterns in data generated by different atmospheric models on various scales and showed their connection to the blocking events in the atmosphere (Majda et al. 2006; Franzke et al. 2007). The strategy they used to identify those hidden patterns(hidden

Markov model with Gaussian output or HMM-Gauss) implies the following assumptions on the underlying data: (i) the hidden process switching between the metastable states is Markovian (i. e. has no long term memory-effects) and (ii) the observed process in each of the metastable states is Gaussian and there is no causal dependence between the consecutive observations (the data points are assumed statistically independent of each other). Of particular interest in the present context is also the numerical scaling of the Expectation-Maximization framework which the HMM-Gauss strategy is based on : (1) it scales as  $\mathbf{O}(n^3)$  w.r.t. the dimension  $n$  of the corresponding phase space of observation data (this reduces the applicability of the method to low-dimensional cases) and (2) it scales as  $\mathbf{O}(K^2)$  w.r.t. the number  $K$  of the hidden states (3) the results are not unique since the EM-strategy finds only the local optima of the corresponding likelihood function (Baum 1972). On the other hand, the HMM-Gauss method scales linearly w.r.t the length of the time series thus making it possible to analyze very long time series.

The first attempts to develop generalizations of the HMM-Gauss approach that are more widely applicable resulted in construction of the following methods: (a) Wavelets-PCA (Horenko and Schuette 2007) (b) HMM-PCA (hidden Markov models with principal component analysis)(Horenko et al. 2006; Horenko and Schuette 2007) and (c) HMM-PCA-SDE (hidden Markov models with principal component analysis and stochastic differential equations) (Horenko et al. 2008).

Wavelets-PCA is an "assumptions free" approach, which means that no a priory knowledge about the properties of the underlying process is needed to identify the hidden persistent phases. The method is based on the minimization of the functional describing the weighted distance between the observed data and their projections on a finite set of  $K$  linear manifolds.

As a result, the method provides the probabilities with which the data points can be assigned to  $K$  hidden states characterized by  $K$  specific sets of essential dimensions. However, the numerical cost of the method is scaling quadratically with number of transitions between the hidden states which seriously restricts the applicability of the method to the relatively short time series with few ( $\approx 10 - 20$ ) transitions between the hidden states (Horenko and Schuette 2007).

The HMM-PCA is based on the same idea (the minimization of the distance functional) as the Wavelets-PCA method except for two additional assumptions made for the analyzed data: (1) the process switching between the metastable states is assumed to be Markovian and (2) in each of the metastable states the projections of the data onto the dominant state-specific dimensions are Gaussian. Compared with the HMM-Gaussian-approach, from the point of view of the assumptions done the HMM-PCA allows only to weaken the constraint regarding the Gaussianity of the observed process in all of the dimensions. However, concerning the numerical gains of the method, it scales as  $k \mathbf{n} \log(\mathbf{n})$  where  $n$  is the observation dimension and  $k \ll n$  is the number of principal components (since instead of the full covariance matrix inversion as in HMM-Gaussian-method, HMM-PCA requires only the identification of  $k$  dominant eigenvectors, which can be achieved applying Raley-Ritz or Lanczos methods). This property together with linearity of the method w.r.t. the length of the time series make HMM-PCA applicable for analysis of high-dimensional time series. However, the Markov-assumption about the hidden process restricts the applicability of the method to data without memory.

If the structure of the data allows some insight into the type of the underlying dynamics, e. g., the type of the noise process (additive or multiplicative), then this additional infor-

mation can be used in the construction of more specific methods of data analysis. As it was demonstrated in our recent paper, one can construct methods combining HMM-PCA with fitting of reduced stochastic differential equations (SDE) (Horenko et al. 2008). As it was demonstrated on the historical temperature data in Europe, the resulting HMM-PCA-SDE-method can be used for predictions and identification of the metastable states even in very high dimensions. However, this method inherits the drawback of the previous methods concerning the non-Markovianity of the analyzed data. Moreover, as it was shown for the temperature data example, the metastability analysis of real meteorological data is "spoiled" with the seasonal trend which results in identification of four seasons as metastable states. The above described numerical problems of the underlying EM-algorithm prohibit reliable identification in the case of many metastable states involved, especially in the cases when the time series are relatively short as it is the case for historical meteorological data.

In the presented paper we describe a hierarchical approach based on successive decomposition of the multidimensional time series in metastable states. Such an approach is especially useful for relatively short but multidimensional time series with many hidden states, since simultaneous identification of all of the hidden states would be hampered by a large uncertainty of the parameter identification and non-uniqueness of the EM-optimization result. The resulting method is capable of dealing with data gaps (resulting from the separation of the data on the previous hierarchical level of analysis). We also demonstrate how to use the idea of extended space representation to cast processes with memory into the Markovian framework (thereby fulfilling the first assumption of the HMM-PCA method). We discuss the assumptions needed for the construction of a new likelihood model of the data with gaps and propose a modified EM-algorithm for log-likelihood optimization. We explain how the

quality of the resulting reduced representation of the data can be acquired, how it can help to estimate the number of the metastable states and what kind of additional information about the analyzed process can be gained. We illustrate the performance of the new method analyzing non-Markovian 500 hPa geopotential height fields (daily mean values from the ERA 40 data set for a period of 44 winters) and compare the outcome to the results obtained with the "Wavelets-PCA" approach. We interpret the results w.r.t. the notion of blocking events in the atmosphere.

# 1. Topological dimension reduction in time series analysis

## *a. Memory in the data and Markovian representation*

Let the observed data be given in the form of a time-discrete sequence  $\{z_t\}_{t=1,\dots,T}$  of  $c$ -dimensional data vectors which describe the observation or measurement of a process at  $T$  subsequent instances. We will say that the process underlying the observations has a memory depth  $d \geq 0$  if the conditional probability distribution  $P$  of future states of the process, given the present state and all past states, depends only upon the present state and  $d$  previous states but not on all past states. Mathematically this property can be expressed as

$$P(z_{t+1}|z_1, z_2, \dots, z_t) = P(z_{t+1}|z_{t-d}, \dots, z_{t-1}, z_t). \quad (1)$$



We will call a process Markovian if  $d = 0$ . For  $D \geq d > 0$  it is obvious, that the extended stochastic process  $x_t^{(D)} = (z_t, z_{t-1}, \dots, z_{t-D})$  (which we will call a  $d$ -frame re-casting of the original process) is Markovian, i. e.

$$P(x_{t+1}^{(D)} | x_1^{(D)}, x_2^{(D)}, \dots, x_t^{(D)}) = P(x_{t+1}^{(D)} | x_t^{(D)}). \quad (2)$$

We will further omit the upper index ( $D$ ) to simplify the notation.

This means that any observed process with finite memory can be cast into the  $Dc$ -dimensional extended space and become Markovian (allowing to apply the Markovian techniques of time series analysis like, e. g., HMMs).

There are two major problems associated with this strategy: (i) reliable estimation of the memory depth  $d$  is not a trivial task if the dimension  $c$  of the observation data is high and (ii) the numerical cost of the time series analysis increases significantly for large  $D$  since the dimension of the extended space is  $D$  times larger than the dimension of the original space.

The first of the above mentioned problems becomes even more serious if the physics of the underlying process is unknown, i. e., if it is not a priory clear what kind of stochastic dynamics should be expected (linear or non-linear, additive or multiplicative noise etc.). Linear approaches, like, e. g., multivariate autoregressive processes (MVAR) (Brockwell and Davis 2002), can be used for estimation of  $d$  in multiple dimensions. However, such kind of analysis does not guarantee the reliability, since there are examples of systems with finite non-linear memory (like, e. g., the time series of stock returns in finance) where linear analysis methods do not reveal any significant memory effects (Tsay 2005). Another problem of such methods is their high numerical cost, the MVAR-method, e. g., scales as  $\mathbf{O}(c^6)$ . This prohibits the application of these methods to very high dimensional systems without making additional

assumptions about the analyzed data (the single dimensions are statistically independent, etc.).

On the other hand, the reported examples of application of non-linear memory estimation methods, like conditional heteroscedastic models (ARCH, (Tsay 2005), or their generalizations), are limited to specific application areas (like econometrics and financial data analysis) and low-dimensional cases, in general they do not allow a robust estimation for very large data sets.

*b. State-specific dimension reduction*

All of the above arguments underline the importance of dimension reduction methods in time series analysis. In order to be able to find hidden metastable states in very high dimensional data, one should be able to couple the problem of the identification of those states to an appropriate dimension reduction strategy. We will now briefly outline the main idea of one of such approaches, the topological dimension reduction (Horenko et al. 2006; Horenko and Schuette 2007; Horenko et al. 2008).

Let us assume that with the help of one of the methods described above, we were able to estimate the upper bound  $D$  of the memory depth for the given time series  $\{z_t\}_{t=1,\dots,T}$ . It is worthy to mention that we do not need to determine the memory depth exactly, since all we are interested in later on is to cast the process into Markovian framework, as it was already explained above. Therefore we need a lower bound on  $D$ . In order to account for memory effects in the analyzed data, we can extend the vector space of observables  $z_t$  at each time  $t$  with  $D$  previous observations  $\{z_{t-1}, \dots, z_{t-D}\}$ . The resulting vector  $x_t = \{z_t, z_{t-1}, \dots, z_{t-d}\}$

is a component in  $n = Dc$ -dimensional space. The idea of the method is to identify the  $m$  principal directions with the highest variance in  $n$ -dimensional data  $x_t$  ( $m \ll n$ ). In contrast to standard PCA, where these principal directions are supposed to be global (i. e. valid for the whole time series  $x_t$ ), the idea of state-specific topological dimension reduction consists in the assumption that the principal directions can vary in time and are defined with the help of a sequence of  $K$  linear projectors  $\mathbf{T}_i \in \mathbb{R}^{n \times m}, i = 1, \dots, K$ , i.e.,  $\mathbf{T}_i$  is understood to project onto the subspace spanned by the local principal directions. Mathematically the problem of identifying  $\mathbf{T}_i$  can be stated as a minimization problem wrt. the residuum-functional, describing the least-squares difference between the original observation and its reconstruction by means of the  $m$ -dimensional projection:

$$\mathbf{L}(x_t, \mathbf{T}_i, \mu_i) = \sum_{i=1}^K \sum_{t=1}^T \gamma_i(t) \left\| (x_t - \mu_i) - \mathbf{T}_i \mathbf{T}_i^\top (x_t - \mu_i) \right\|_2^2, \quad (3)$$

where  $\gamma_i(t)$  (we will further name it the hidden path) denotes the probability to optimally describe the  $n$ -dimensional vector  $x_t$  at time  $t$  with the local projector  $\mathbf{T}_i$  and  $\sum_{i=1}^K \gamma_i(t) = 1$  for all  $t$ . The quantity  $\gamma_i(t)$  provides a relative weight to the statement that an observation  $x_t$  belongs to the  $i$ th hidden state. For the moment we assume the sequence of probabilities  $\gamma_i(t)$  to be known and fixed, in the next section we will present a way to estimate this sequence from a given observation  $x_t$ . The functional  $\mathbf{L}$  depends on the projector matrices  $\mathbf{T}_i$  and center vectors  $\mu_i \in \mathbb{R}^n$ . Moreover, the projectors  $\mathbf{T}_i$  are subject to the orthogonality condition:

$$\mathbf{T}_i^\top \mathbf{T}_i = Id^{m \times m}. \quad (4)$$

The solution of the optimization problem (3) subjected to orthogonality constraints (4) is possible in the three following cases (Horenko and Schuette 2007):

(i) *Case 1 (known hidden path)*

If the hidden path  $\gamma_i(t)$  is known then the minimum of the functional (3) can be found analytically resulting in a state-specific version of the PCA:

$$\left( \sum_{t=1}^T \gamma_i(t) (x_t - \mu_i)(x_t - \mu_i)^\top \right) \mathbf{T}_i = \mathbf{T}_i \Lambda_i, \quad (5)$$

$$\mu_i = \frac{\sum_{t=1}^T \gamma_i(t) x_t}{\sum_{t=1}^T \gamma_i(t)}, \quad (6)$$

where  $\Lambda_i$  is a matrix with  $m$  dominant eigenvalues of the weighted covariance matrix  $\sum_{t=1}^T \gamma_i(t) (x_t - \mu_i)(x_t - \mu_i)^\top$  on the diagonal (non-diagonal elements are zero), i. e. each of the  $K$  hidden states is characterized by a specific set of essential dimensions  $\mathbf{T}_i$  (which can be defined as corresponding dominant eigenvectors) and center vectors  $\mu_i \in \mathbb{R}^n$  calculated from the conditional averaging of the time series wrt. corresponding occupation probabilities  $\gamma_i(t)$  (Horenko et al. 2006).

(ii) *Case 2 (HMM-PCA)*

Let us make the following two assumptions: (i) the unknown sequence of hidden probabilities  $\gamma_i(t)$  can be assumed to be an output of the Markov process  $X_t$  with  $K$  states and (ii) the probability distribution  $P(\mathbf{T}_i x_t | X_t = i)$  (which is the conditional probability distribution of the projected data in the hidden state  $i$ ) can be assumed to be Gaussian in each of the hidden states. If both of these assumptions hold then the HMM-framework can be used and one can construct a special form of EM-algorithm to find the minimum of the residuum-functional (3) (for details of derivation and resulting algorithmic procedure we refer to our previous works (Horenko et al. 2006; Horenko and Schuette 2007)). The resulting

method is linear in  $T$ , scales as  $\mathbf{O}(mn^2)$  with the dimension of the problem and as  $\mathbf{O}(K^2)$  with the number  $K$  of the hidden states. However, as all of the likelihood-based methods in HMM-setting, HMM-PCA does not guarantee the uniqueness of the optimum since the EM-algorithm converges towards a local optimum of the likelihood-function.

(iii) *Case 3 (Wavelets-PCA)*

both of the HMM-PCA model assumptions are very difficult to check (especially for high dimensional data), therefore we need to construct a method being free of those assumptions and which we can use for a posteriori verification of the HMM-PCA results. Therefore, we assume that the unknown function  $\gamma_i(t)$  can be represented as a finite linear combination of (few) discrete Haar-wavelet functions  $\phi(x)$

$$\phi(x) = \xi_{[0,1)} = \begin{cases} 1 & 0 \leq x < 1 \\ 0 & \text{any other} \end{cases} \quad (7)$$

With their help any hidden occupation probability function  $\gamma_i(t) \in \mathbf{L}_2(\mathcal{R})$  on any given scale  $J \in \mathcal{Z}$  can be represented by a respective scale-specific projection

$$\begin{aligned} P_J \gamma_i(t) &= \sum_{r \in \mathcal{Z}} c_r^i \phi(2^J t - r) \\ c_r^i &= \int_0^1 \gamma_i(2^{-J}(r + s)) ds \end{aligned} \quad (8)$$

If the number of the ansatz functions in expansion (8) can be assumed to be small, it allows to project the original high-dimensional optimization problem to the low-dimensional space of the wavelet coefficients  $c_r^i$ . The integral transformation between the wavelet representation and the occupation probabilities  $\gamma_i(t)$  can be efficiently implemented using the fast Haar-wavelet transformation (FWT) (Strang and Nguyen 1997).

In our specific implementation of the wavelet-based optimization procedure (Horenko and Schuette 2007), we made two simplifying assumptions: (i) we assumed that the occupation probability functions  $\gamma_i(t)$  can take only discrete values 0 and 1 (i. e. the occupation probabilities are assumed to be discrete step functions) and (ii) we fixed the upper limit of the Galerkin subspace dimension for each of the optimization runs (i. e., together with the assumption (i) it means that we set the upper limit of transitions between  $K$  hidden states).

The main advantage of the resulting Wavelet-PCA approach is that it is independent of the model assumptions (Markovianity and Gaussianity) of the HMM-PCA method. However, our specific implementation of the method scales quadratically with the number of involved Haar-wavelet functions, i. e. the method can not be used to get reliable results for very long time series with large number of transitions between the hidden states. But it can be used for validation of the model assumptions of the HMM-PCA by comparison of the  $\gamma_i(t)$  values identified by both methods for relatively short segments of the analyzed time series.

## 2. Hierarchical approach

As it was demonstrated above, the application of the Hidden Markov framework for HMM-PCA approach results in a specific assumption about causal dependence inside of the data series. It means that the construction of the likelihood function implies that (i) the data sequence being subjected to the HMM-PCA analysis has to be contiguous and (ii) the time intervals between the consecutive observations should be equal (Horenko et al. 2006). Whereas the assumption (ii) is usually satisfied for most of the available data sets, assumption (i) is much more restrictive since there are a lot of processes which cannot be

permanently observed (f. e. the financial data are available only during the trading sessions on the stock market and are not available on weekends and holidays). The assumption (i) will also prohibit the application of the HMM-PCA in the case when one is interested in analyzing only specific segments of available data (f. e. the meteorological data restricted to certain seasons) or if the time series is subjected to hierarchical decomposition into metastable substates. It is worthy to mention that one can still apply the Wavelets-PCA method in all of this cases but as it was already mentioned above, the applicability of Wavelets-PCA is restricted to the cases where only few transitions between the hidden states are present.

Therefore, we are interested in extension of the HMM-PCA framework towards the cases where there are gaps in observation sequence where the causal dependence implied by Markovian picture is broken. In order to cast the description of the data into the HMM framework, we first define the complete observation set  $\mathcal{X}_t = (X_t, x_t)$ , where  $X_t$  is an output of some unobserved (or hidden Markov chain) and  $x_t$  is observed data. We will further assume that (a) the observation data  $\{x_t\}_{t=1,\dots,T}$  consists of a sequence of  $N_{traj}$  contiguous observation sequences  $x^i$  (i. e.  $\{x_t\}_{t=1,\dots,T} = \{x^1, x^2, \dots, x^{N_{traj}}\}$ ), that (b) the time intervals between subsequent observations in each of the contiguous data sequences are equal and that (c) the gaps between the neighboring data sequences are so big that each consecutive data sequence can be assumed to be statistically independent from the predecessor sequence. We will refer to the original time series as data sequence, whereas the contiguous segments of it with time equidistant observations will be called subsequences. The last assumption (c) means that the following relation is valid for a joint conditional probability distribution

function  $P(\mathcal{X}_t|\lambda)$  (also called likelihood):

$$P(\mathcal{X}_1, \mathcal{X}_2, \dots, \mathcal{X}_T|\lambda) = \prod_{l=1}^{N_{traj}} P(\mathcal{X}_{t_1^l}, \dots, \mathcal{X}_{T^l}|\lambda). \quad (9)$$

where  $\lambda = (\pi, A, \mu_1, \mathbf{T}_1, \dots, \mu_K, \mathbf{T}_K)$ ,  $A$  is the transition matrix of the hidden Markov process  $X_t$ ,  $\pi$  is the invariant distribution of initial states of the hidden process and  $(\mu_i, \mathbf{T}_i)$  are parameters of essential linear manifolds characteristic for each of the hidden states.  $t_1^l$  and  $T^l$  define the start and the end of the contiguous subsequence  $l$  inside of the observation data.

We define the log-likelihood functional of the process as

$$\begin{aligned} \mathbf{L}^{\log}(\lambda|\mathcal{X}) &= \log P(\mathcal{X}_1, \mathcal{X}_2, \dots, \mathcal{X}_T|\lambda) = \\ &= \sum_{l=1}^{N_{traj}} \mathcal{L}(\lambda|\mathcal{X}_{t_1^l}, \dots, \mathcal{X}_{T^l}). \end{aligned} \quad (10)$$

where  $\mathcal{L}$  are standard HMM-PCA log-likelihood functions for contiguous time series with observations equidistant in time (Horenko et al. 2006).

We employ the EM algorithm to maximize both likelihood and log-likelihood functions simultaneously. Starting with some initial model  $\lambda_0$ , we iteratively refine the model within two steps:

- The Expectation-step: In this step the state occupation probability  $\gamma_t^l(i) = P(X_t = i | x_t, \lambda)$ , and the transition probability  $\eta_t^l(i, j) = P(X_t = i, X_{t+1} = j | x_t, \lambda)$ , are calculated for each time  $t \in [t_1^l, \dots, T^l]$ , given the observation  $x_t$  and the current model  $\lambda$ . In order to calculate the two conditional probabilities of the **E-step**, we first define two additional variables

$$\alpha_t^l(i) = P(x_{t_1^l} \dots x_t, X_t = i | \lambda) \quad (11)$$



and

$$\beta_t^l(i) = P(x_{t+1}x_{t+2}\dots x_{T^l} \mid X_t = i, \lambda), \quad (12)$$

where  $\alpha_t^l(i)$  and  $\beta_t^l(i)$  are forward- and backward-variables respectively. The interpretation of  $\alpha_t^l(i)$  is as follows: it denotes the probability of the observation subsequence  $l$  up to time  $t$  together with the information that the system is in hidden state  $i$  at time  $t$  conditioned wrt. the given model parameters  $\lambda$ . The following formulas show that the computation of the sequence  $\alpha_t^l(i)$  for the whole sequence is possible with  $K^2 T$  operations:

$$\alpha_{t_1}^l(i) = \pi_i \rho_i(x_{t_1}^l), \quad 1 \leq i \leq K \quad (13)$$

$$\alpha_{t+1}^l(j) = \left[ \sum_{i=1}^K \alpha_t^l(i) A_{ij} \right] \rho_j(x_{t+1}), \quad (14)$$

$$1 \leq t \leq T-1, 1 \leq j \leq K. \quad (15)$$

where  $\rho_j(x_{t+1}) = \rho(x_{t+1} \mid X_{t+1} = j)$  defines the conditional observation probability of the data at time  $t+1$  in the hidden state  $j$ . The backward variable  $\beta_t^l(i)$  can be computed with analogous formula:

$$\beta_{T^l}^l(i) = 1, 1 \leq i \leq K \quad (16)$$

$$\beta_t^l(i) = \sum_{j=1}^K A_{ij} \rho_j(x_{t+1}) \beta_{t+1}^l(j), \quad (17)$$

$$t = T^l - 1, T^l - 2, \dots, 1, 1 \leq i \leq K \quad (18)$$

$$P(x_{t_1}^l \mid \lambda) = \sum_{i=1}^K \beta_1^l(i) \pi_i \rho_i(x_{t_1}^l) \quad (19)$$

From (11) and (12) one can finally compute the probability for all  $t$  as

$$P(x_t | \lambda) = \sum_{i=1}^K \alpha_t^l(i) \beta_t^l(i), \quad (20)$$

where  $l$  is chosen in such a way that  $t \in [t_1^l, \dots, T^l]$ . The two conditional probabilities of the **E-step** can be calculated efficiently by using the forward-backward variables:

$$\eta_t^l(i, j) = \frac{\alpha_t^l(i) A_{ij} \rho_j(x_{t+1}) \beta_{t+1}^l(j)}{P(x_t | \lambda)}. \quad (21)$$

With these values the probability to be in state  $i$  at time  $t$  can be expressed as

$$\gamma_t^l(i) = \sum_{j=1}^K \eta_t^l(i, j). \quad (22)$$

Note that the expected number of transitions from  $i$  to any other state (including itself) within the whole observation is  $\sum_{l=1}^{N_{tra}} \sum_{t=t_1^l}^{T^l-1} \gamma_t^l(i)$ , and the expected number of transitions from  $i$  to  $j$  is  $\sum_{l=1}^{N_{tra}} \sum_{t=t_1^l}^{T^l-1} \eta_t^l(i, j)$ .

- The Maximization-step: This step finds a new model  $\hat{\lambda}$  via a set of reestimation formulas. The maximization guarantees that the likelihood does not decrease in each single iteration.

In order to apply the EM-algorithm, we need to re-estimate parameters  $\lambda$  describing the hidden Markov model and essential linear manifolds via the maximum likelihood estimator. Hereby, the observation  $x_t$  at time  $t \in [t_1^l, \dots, T^l]$  has to be weighted with the probability for the hidden state  $i$   $\gamma_t^l(i)$  for the respective subsequence  $l$ . In order to calculate this re-estimation formulas we fix the sequence  $X_t$  of the hidden states (this means also keeping the sequence of  $\gamma_t^l(i)$  fixed) and calculate the derivatives of the functional (10) wrt. the parameter set  $\lambda$ . Setting all of the partial derivatives to

zero for some fixed reduced dimensionality  $m$  we get a coupled system of nonlinear algebraic equations for the parameters which can be solved analytically analogous to the derivation shown in (Horenko et al. 2006; Horenko and Schuette 2007). We will skip the derivation here and just present the final re-estimation formulas

$$\mu_i = \frac{1}{\sum_{l=1}^{N_{traj}} \sum_{t=t_1^l}^{T^l-1} \gamma_t^l(i)} \sum_{l=1}^{N_{traj}} \sum_{t=t_1^l}^{T^l-1} \gamma_t^l(i) x_t, \quad (23)$$

$$\text{Cov}_i \mathbf{T}_i = \mathbf{T}_i \max_m (\text{spec}(\text{Cov}_i)), \quad (24)$$

where  $\max_m (\text{spec}(\text{Cov}_i))$  denotes  $m$  dominant eigenvalues of the covariance matrix  $\text{Cov}_i$ :

$$\text{Cov}_i = \frac{1}{\sum_{l=1}^{N_{traj}} \sum_{t=t_1^l}^{T^l-1} \gamma_t^l(i)} \sum_{l=1}^{N_{traj}} \sum_{t=t_1^l}^{T^l-1} \gamma_t^l(i) (z_t - \mu_i)(z_t - \mu_i)^\top, \quad (25)$$

The E- and M-steps are iteratively repeated until a predetermined maximal number of iterations is reached or the improvement of the likelihood becomes smaller than a given limit. The entire EM algorithm has the nice property that the likelihood function is non-decreasing in each step, i.e., we iteratively approximate local maxima. We will call the presented method ensemble HMM-PCA to refer to the ability of the new method to deal with an ensemble of statistically independent subsequences and to stress the difference with the standard HMM-PCA. As for the scaling of numerical effort, the resulting ensemble HMM-PCA method is linear in the length of the observation series  $x_t$ , quadratic in the number  $K$  of hidden Markov states (essentially since the transition matrix elements of the hidden Markov chain should be estimated), and scales as  $\mathcal{O}(mn^2)$  in the reduced dimensionality  $m$  (since only  $m$  dominant eigenvectors of  $\text{Cov}_i$  matrix are required, they can be obtained with numerically efficient

subspace methods like Rayleigh-Ritz-iteration or Lanczos method). Therefore the ensemble HMM-PCA approach is applicable to systems with very high dimensionality and very long observation data sequences. This feature is demonstrated in Section 5 where the method is used for analysis of the multidimensional meteorological data-set.

### 3. Estimation of confidence intervals and choice of $K$

It is intuitively clear that the quality of the resulting reduced model is very much dependent on the original data, especially on the length of the available time series. The shorter is the observation sequence, the bigger is the uncertainty of the resulting parameters. The same is true if the number  $K$  of the hidden states is increasing for the fixed length of the observed time series: the bigger is  $K$ , the higher will be the uncertainty for each of the states. Therefore in order to be able to statistically distinguish between different hidden states we need to get some notion of the HMM-PCA robustness. This can be achieved through the estimation of confidence intervals for the both parts of the model: for the hidden Markov process and the extended EOFs.

#### *(iv) Hidden Markov process*

In order to estimate the confidence intervals of the hidden transition probabilities  $A_{ij}$  we first make use of the second derivatives  $\frac{\partial^2 \mathbf{L}}{\partial A_{ij}^2}(\bar{A})$  (also called Fisher information) of the

log-likelihood function (10) subjected to the constraint

$$\sum_{j=1}^K A_{ij} = 1, \quad \forall i = 1, \dots, K. \quad (26)$$

$\bar{A}$  is the hidden transition matrix of the Markov chain estimated by the HMM-PCA algorithm. We denote the number of the transitions in the identified Markovian sequence  $X_t$  between the states  $i$  and  $j$  as  $N_{ij}$ . The most probable sequence  $X_t$  of the hidden states can be directly computed from the hidden probabilities  $\gamma_t^l(i)$  applying, f. e., the Viterbi-algorithm (Viterbi 1967). Then it is easy to verify that the explicit expression for the Fisher information of the identified Markov chain  $X_t$  is

$$\frac{\partial^2 \mathbf{L}^{\log}}{\partial A_{ij}^2}(\bar{A}) = -\frac{\left(\sum_{k=1}^K N_{ij}\right)^2}{N_{ij}}. \quad (27)$$

Then the confidence intervals of the hidden Markov process are given by  $(\bar{A}_{ij} - \delta(\bar{A}_{ij}), \bar{A}_{ij} + \delta(\bar{A}_{ij}))$ , where

$$\delta(\bar{A}_{ij}) = 1.96 \left( -\frac{\partial^2 \mathbf{L}^{\log}}{\partial A_{ij}^2}(\bar{A}) \right)^{-0.5}, \quad (28)$$

and multiplier 1.96 comes from the definition of 95% confidence interval in Gaussian statistics.

(v) *Extended EOFs*

The Gaussianity assumption for the observation process in the HMM-PCA-method gives an opportunity to estimate the confidence intervals of the manifold parameters  $(\mu_i, \mathbf{T}_i)$  straightforwardly. This can be done in a standard way of multivariate statistical analysis since the variability of the weighted covariance matrices (25) involved in the calculation

of the optimal projectors  $\mathbf{T}_i$  is given by the Wishart distribution (Mardia et al. 1979). The confidence intervals of the  $\mathbf{T}_i$  can be estimated by sampling from this distribution and calculating the  $m$  dominant eigenvectors of the sampled matrices, whereas the confidence intervals of  $\mu_i$  can be acquired from the respective standard deviations (Mardia et al. 1979).

*(vi) Optimal choice of  $K$*

If there exist two states with confidence intervals overlapping for each of the respective reduced model parameters, then those are statistically indistinguishable,  $K$  should be reduced and the HMM-PCA calculation repeated. In other words, confidence intervals implicitly give a natural upper bound for the number of hidden states. On the other hand, the spectral theory of the Markov processes connects the number  $K$  of metastable states with the number of the dominant eigenvalues in the so called Perron cluster (Schütte and Huisinga 2003). This allows to apply the Perron cluster - cluster analysis (PCCA) (Deuffhard and Weber 2005) to find the lower bound of  $K$ . Both these criteria in combination can help to find the optimal number  $K$  of the hidden states in each specific application.

## 4. Analysis of the hidden transition matrix

Application of the HMM-PCA-algorithm to the analyzed multidimensional data results in a two-fold dimension reduction: besides the identification of dominant local extended orthogonal functions describing the directions of maximal data-variability, HMM-PCA reveals a hidden discrete Markov process switching between different sets of those extended EOFs.

Analysis of the corresponding hidden transition matrix  $A$  can help to understand the global properties of the underlying multidimensional dynamics which is now given by the series of one-dimensional discrete hidden variable  $X_t$ . We will now briefly sketch some of those properties and explain how to calculate them. For more details we refer to a standard literature on Markov chains, f. e., (Gardiner 2004).

*(vii) Relative statistical weights*

Vector  $\pi$  of relative statistical weights of the hidden states can be calculated as the fix-point of the Markovian transition operator, i. e.,

$$\pi = \pi A. \tag{29}$$

Note that we use the multiplication from the left since  $A$  is the stochastic matrix with row sums all equal to 1.0.

*(viii) Mean exit times*

Mean exit time  $\tau_i^{ex}$  is the expected time for the process  $X_t$  to stay in the hidden state  $i$  until it switches to any other state. Thus it is one of the basic quantities and can be used to compare different hidden states wrt. their metastability. It can be directly computed from the diagonal elements of the transition matrix  $A$

$$\tau_i^{ex} = \frac{\delta t}{1 - A_{ii}}, \tag{30}$$

where  $\delta t$  is the time step between the observations.

(ix) *Mean first passage times*

For any pair of two different hidden states  $i$  and  $j$ , mean first passage time  $\tau_{ij}^{pas}$  represents the expected time for the process  $X_t$  to start in the state  $i$  and to reach the state  $j$  for the first time. It can be calculated from the solution of the following linear system of equations:

$$\tau_{ij}^{pas} = \begin{cases} \delta t + \sum_{k=1}^K \tau_{kj}^{pas} A_{ik}, & i \neq j, \\ 0, & i = j. \end{cases} \quad (31)$$

This quantity describes the dynamical properties of the process  $X_t$  and can be used to analyze and compare different transition pathways between metastable states.

## 5. Analysis of historical geopotential height data

*a. Description of the data*

Using the method presented in the previous sections, we analyze daily mean values of the 500 hPa geopotential height field from the ERA 40 reanalysis data (Simmons and Gibson 2000). We consider a region with the coordinates: 27.5° W – 47.5° E and 32.5° N – 75.0° N, which includes Europe and a part of the Eastern North Atlantic. The combination of land and sea makes the selected region preferable for the appearance of dynamically relevant phenomena and it captures the area of maximum Atlantic block formation (Wiedenmann et al. 2002). The resolution of the data is 2.5° which implies a grid with 31 points in the zonal and 18 in the meridional direction. We have also tested the sensitivity of the results presented here by reducing the resolution by a factor of two taking only 16 × 9 grid points.



For the analysis we have considered geopotential height values only for winter and for the period 1958/59 till 2001/02, where a winter includes the months December to February, thus we end with a not equidistant time series of 3960 days. The reason for considering winter months only was first: due to the increased equator-to-pole temperature gradient the synoptic eddies and the quasi-stationary Rossby waves in the atmosphere are much more intense during winter, this suggests much more pronounced regime behavior, and second: if we focus on blocking events only, representing a kind of metastability in the circulation – there is a pronounced maximum in the block formation for the considered region during winter (Lupo et al. 1997).

We have mentioned already in the introduction the problem with the seasonal cycle when analyzing atmospheric data wrt. metastable behavior. In order to remove the seasonal trend we apply a standard procedure, where from each value in the time series we subtract a mean build over all values corresponding to the same day and month e.g., from the data on 01.01.1959 we subtract the mean value over all days which are first of January and so on.

*b. The Blocking index*

For the purpose of interpreting the results of the presented method wrt. metastability of blocking events we compute the Lejenas-Okland index from the data. It indicates the appearance of a blocking anticyclone and the duration of the event. We have a blocking if the geopotential height difference at 500 hP between  $40^\circ$  N and  $60^\circ$  N is negative over a region with  $20^\circ$  zonal extent. The exact formula is given in (Lupo et al. 1997), for the purpose of representation we have computed a zonally averaged value of the index, rescaled

it and reversed its sign. A part of the time series of the index is shown in Fig. 9.

*c. Discussion of the results*

In order to choose the lower bound of the frame length in the algorithm, the memory depth of the data was estimated from the autocorrelation and partial autocorrelation function. The dominant eigenvalues of the autocorrelation matrix and of the autoregressive (AR) coefficients computed at different time lags are presented in Fig.1. From the spectrum of the AR coefficients one can see that the data has an internal memory of about five days and it can be approximately modeled by an autoregressive process (AR) of the order 5, the oscillations after the fifth day are interpreted as noise. We conclude that a frame length of 5 days will be sufficient to make the data Markovian.

To choose the optimal number of hidden states  $K$  we first start the HMM-PCA algorithm with  $K = 8$  for different values of  $d = 1, 5, 10, 20, 40$  and  $m = 1$ . As it was mentioned above, since only relatively short time series is available (with approx. 4.000 data points), we need first to estimate the upper bound for  $K$  comparing the confidence intervals of HMM-PCA parameters. In order to avoid the inherent problem of EM-algorithm, namely that it only converges to the local maximum of the likelihood functional (dependent on the initial parameter values), we perform the optimization with different randomly chosen sets of initial parameters 100 times and take the result with maximal likelihood. One of the transition matrix spectra is shown in Figure 2. If the confidence intervals for a pair of states are overlapping it means that the corresponding states are statistically undistinguishable and the whole optimization procedure should be repeated for  $K = K - 1$ . It comes out that

only for  $K = 4$  all of the hidden states are statistically distinguishable, therefore we proceed further with 4 hidden states.

As next, we have to verify the assumptions needed to apply the HMM-PCA method. The first possibility is to a posteriori check the Gaussianity of the data in the hidden states and Markovianity of the hidden process. However, it will not guarantee that these assumptions will also be fulfilled in any of the EM-iterations. Another possibility is to compare the results of the HMM-PCA optimization with, f. e., some fragment of Wavelets-PCA results (since Wavelets-PCA is much slower but does not imply any assumptions on the analyzed data). This will give us a possibility to estimate the robustness of optimization wrt. the model assumptions. As we see from the Figure 3, the respective Viterbi-paths are almost identical for both of the methods, therefore it verifies the usage of the HMM-PCA analysis.

Next we have studied the sensitivity of the results wrt. different frame lengths. The calculated Viterbi paths, showing the most probable sequence of hidden states, are displayed in Figure 4. When the frame length increases, the transitions between the hidden states reduce and the occupation duration increases. The discrepancy of the Viterbi paths for different frame lengths can be due to the fact that the data with the smaller frame length is non-Markovian but the algorithm can still find some metastable regime behavior, which is filtered out if the larger frame length is applied.

We have tested the dependence of the results on the resolution, using data on a  $16 \times 9$  and on a  $32 \times 18$  grid for the analysis. The Viterbi paths for both grids are shown in Figure 4 and they are nearly identical. Figures 5 and 6 display the center vectors  $\mu_i$  for the two different resolutions and  $d = 1$ . In both cases the large scale structure of the pattern is captured by the algorithm.

From the Figures we see that the hidden states describe two different regimes:  $\mu_1$  and  $\mu_3$  are characterized by a negative geopotential anomaly at higher latitudes and a positive anomaly at lower latitudes, whereas the other two states  $\mu_2$  and  $\mu_4$  have the reversed sign of the anomalies. Thus the states in the first regime are associated with an intensification of the zonal flow and those in the second regime with weakening. Each regime can be then subdivided into states with stronger anomaly:  $\mu_3$  and  $\mu_4$  and those with weaker anomaly  $\mu_1$  and  $\mu_2$ .

We expect that blocking events will be captured mostly by the hidden state 4 and this is confirmed if we plot the probability  $\gamma_4$  and the blocking index, see Figure 9. Comparing the Viterbi paths and the blocking index we calculated that state 4 and state 2 capture 46 % and 36 % of all blocking events. If we consider as blocking situations where the blocking index is negative over a period larger than 6 days (filtered index), the numbers above change to 58 % and 29 %, respectively. Looking at individual events we found that the two states represent also other weather patterns with an anomalous geopotential gradient, e.g., cut-off lows. Nevertheless about 73 % of all days in state 4 are associated with blockings, for state 2 this number is 47 %. If we consider the filtered blocking index the numbers change to 52 % and 21 %, respectively.

But how do the results change when we make the data Markovian considering an extended space with the dimension  $n = d * c$ ? We can split the center vector  $\mu_i$  into  $d$  parts with the original dimension  $c$ , representing the mean state of the system at different time lags. The resulting sequence can be interpreted as the "mean time evolution" of the mean state in  $i$ . Figure 10 displays such an sequence for  $\mu_4$ , it shows the growth in time of the meridional geopotential gradient anomaly.

In order to represent the results for larger frame lengths and different states, we have computed the geopotential height difference between 40° N and 60° N from the vector  $\mu_i$  at different time lags, using exactly the same criteria as for the calculation of the blocking index (see Section b), but now we consider all values, not only the negative one. The results are displayed in Figure 11. We see that the overall time evolution is characterized by a growth or a decay of the meridional geopotential gradient which for  $q = 5$  reaches at the end its values from the analysis with  $q = 1$ . For larger frame lengths the amplitude of the gradient is strongly reduced but the time evolution shows more complex character: changing phases of decay and growth, e.g., state four in the case of  $q = 40$ . This can be probably explained by the fact that since in those cases the duration of the blocking is compared with or smaller than a dynamical frame length  $d$ , many creations/destructions of the blocking situations are getting averaged out.

As the proposed techniques for frame lengths  $\geq 2$  is a special type of time-lagged statistics, it can be used to study onsets and withdrawal of diagnosed features. In this, given a time lag  $q$ , we have computed conditional composites for diagnosed events. For onsets, we have selected time slices  $t_j$ ,  $j = j_1, j_2, \dots, j_{N_e}$  ( $N_e$  is the number of diagnosed events) when the occupation probability for the state 4  $\gamma_4^l$  reaches unity. This state was selected because it corresponds most closely to blockings as diagnosed by the employed blocking index. An additional condition is imposed that  $\gamma_4^l$  remains unity at least for five consequent days ( a condition of persistence). For these time slices, a conditional average is computed.

$$x^o(q) = \frac{\sum_{t_j=1}^{N_e} \gamma_{4,t_j-q}^l x_{t_j-q}}{\sum_{t_j=1}^{N_e} \gamma_{4,t_j-q}^l}. \quad (32)$$

An analogous conditional average is computed for withdrawals by selecting the time slices  $t_k$ ,  $k = k_1, k_2, \dots, k_{N_e}$  as the last days of the diagnosed events when  $\gamma_4^l = 1$ . After that, a conditional average for withdrawals is computed

$$x^w(q) = \frac{\sum_{t_k=1}^{N_e} \gamma_{4,t_k-q}^l x_{t_k-q}}{\sum_{t_k=1}^{N_e} \gamma_{4,t_k-q}^l}. \quad (33)$$

In both cases  $q = 0, \dots, d - 1$ , where  $d$  is the frame length.

We note different interpretations of  $x^o(q)$  and  $x^w(q)$ . In the former case,  $q$  covers time interval before the block onset. As a result, the composite  $x^o(q)$  corresponds to typical synoptical conditions before the block onset. In contrast, for  $x^w(q)$ ,  $q$  covers time moments when block exists and, generally, well developed. As a result,  $x^w(q)$  has to be interpreted as a typical pattern of mature blocking state.

For onsets, the composite pattern exhibits developing meridional wavy structure (Figure 7). This feature first appears in the south-western part of the studied domain as a positive anomaly of geopotential height ( $q = 4 - 2$ ). Afterwards, at  $q = 1 - 0$  this anomaly spreads to the east and becomes more pronounced forming a ridge (a trough) in the southern (northern) part of the domain. Eventually, these trough-ridge system evolves to the blocked state. These features are common for the development of typical Atlantic blocking (Berggren et al. 1949; Rex 1950a; Diao et al. 2006).

For withdrawals (Figure 8), we see very marked positive anomaly of geopotential height in the southern part of the domain and negative in the northern part. Both of these anomalies does not move for different values of  $q$  within this composite. This emphasises a stationarity of blockings within their life cycles. However, it becomes more marked if one travels from  $q = 4$  to  $q = 0$ . The reason for this is due to the chosen length of frame, 5 days, which is

comparable to the typical duration of blockings (e.g., (Rex 1950b; Wiedenmann et al. 2002; Lupo et al. 1997; Diao et al. 2006; Croci-Maspoli et al. 2007)). The fully developed anomaly spreads above the most part of the northern Atlantic and attains large magnitude.

Next we analyze the hidden transition matrix identified by the HMM-PCA in Markovian case ( $K = 4, m = 1, d = 5$ ). The transition graph correspondent to the identified matrix  $A$  is shown in Figure 12. Each of the hidden states corresponds to a dynamical pattern of 5 days. As we have seen above in Figure 11, each of the patterns is associated with specific blocking formation or destruction events. Therefore analyzing the transition graph from Figure 12 we can gain some insight into kinetics of such events. We start with the calculation of relative statistic weights of the respective hidden states. Solution of (29) yields  $\pi_1 = 0.2363, \pi_2 = 0.1836, \pi_3 = 0.4234, \pi_4 = 0.1567$ , i. e. the dynamical pattern correspondent to the blocking formation in hidden state 4 is the most seldom one. To compare the metastability of the hidden states, we can calculate the mean exit times  $\tau_i^{ex}$  from (30). We get the following values:  $\tau_1^{ex} = 4.3, \tau_2^{ex} = 5.3, \tau_3^{ex} = 14$  and  $\tau_4^{ex} = 16$  days. Together with Figure 12 it can be interpreted in such a way that both 3 and 4 are metastable states, whereas 1 and 2 correspond to a transition pathway between them. Blocking events associated with the hidden state 4 represent a metastable event in Markovian picture, its typical duration is 16 days and two typical transition pathways in the system are  $3 \rightarrow 1 \rightarrow 2 \rightarrow 4$  and  $4 \rightarrow 2 \rightarrow 1 \rightarrow 3$ . To characterize and to compare these two pathways we calculate the mean first passage times. As results from (31),  $\tau_{34}^{pas} = 131$  and  $\tau_{43}^{pas} = 49$  days, i. e., it takes much longer to “create” a blocking situation then to “destroy” it. This is also in a good acquaintance with respective statistical weights  $\pi$  of the corresponding states, since the “un-blocked” metastable state 3 is visited almost 3 times more frequently then the

“blocked” state 4.

## 6. Conclusion

We have presented a numerical framework for the simultaneous identification of hidden states and respective essential orthogonal functions (EOFs) in high-dimensional data with gaps. It allows to construct reduced representation of analyzed data in the form of a discrete Markov-jump process switching between different sets of EOFs. We discussed the model assumptions and explained the necessity of combining different methods relying on separate sets of model assumptions for data-analysis.

We have also demonstrated what kind of additional insight into underlying dynamics can be gained from a reduced Markovian representation, f. e., in the form of transition probabilities, statistical weights, mean first exit times and mean first passage times. The proposed pipeline of data-analysis based on HMM-PCA was exemplified on analysis of 500 hPa geopotential height fields in winter. Correspondence between the hidden probability in one of the metastable states and the zonally averaged blocking index was found, the respective mean dynamical patterns in the hidden states were found to be describing the creation and destruction of the blocking situations.

One of the basic problems of the multivariate meteorological data is that only relatively short fragments of the observation process are available for the analysis. Therefore it is very important to be able to extract the reduced description out of the data and to control the sensitivity of the HMM-PCA analysis wrt. the length of the time series and the number  $K$  of the hidden states. We gave some hints for selection of optimal  $K$  and explained how the



quality of the resulting reduced representation can be acquired.

### *Acknowledgments*

We are thankful to H. Oesterle who provided us with the ERA 40 reanalysis data from the European Center for Medium-Range Weather Forecasting. Illia Horenko's contribution was supported by the DFG research center MATHEON "Mathematics for key technologies" in Berlin, Stamen Dolaptchiev and Rupert Klein's contributions were partially supported by Deutsche Forschungsgemeinschaft, Grant KL 611/14.

## REFERENCES

- Baum, L., 1972: An inequality and associated maximization technique in statistical estimation for probabilistic functions of Markov processes. *Inequalities*, **3**, 1–8.
- Benzi, R., G. Parisi, A. Suter, and A. Vulpiani, 1982: Stochastic resonance in climatic change. *Tellus*, **3**, 10–16.
- Berggren, R., B. Bolin, and C. G. Rossby, 1949: An aerological study of zonal motion, its perturbations and break-down. *Tellus*, **1**, 14–37.
- Brockwell, P. and R. Davis, 2002: *Introduction to Time Series and Forecasting*. Springer, Berlin.
- Charney, J. G. and J. G. Devore, 1979: Multiple flow equilibria in the atmosphere and blocking. *Journal of Atmospheric Sciences*, **36**, 1205–1216.
- Cheng, X. and J. M. Wallace, 1993: Cluster analysis of the northern hemisphere wintertime 500-hpa height field: Spatial patterns. *Journal of Atmospheric Sciences*, **50**, 2674–2696.
- Corti, S., F. Molteni, and T. N. Palmer, 1999: Signature of recent climate change in frequencies of natural atmospheric circulation regimes. *Nature*, **398**, 799–802, doi:10.1038/19745.
- Croci-Maspoli, M., C. Schwierz, and H. Davies, 2007: A multifaceted climatology of atmospheric blocking and its recent linear trend. *J. Climate*, **20**, 633–649.

- Deuffhard, P. and M. Weber, 2005: Robust Perron cluster analysis in conformation dynamics. *Lin. Alg. App.*, **398c**, 161–184.
- Diao, Y., J. Li, and D. Luo, 2006: A new blocking index and its application: blocking action in the northern hemisphere. *J. Climate*, **19**, 4819–4839.
- Efimov, V. V., A. V. Prusov, and M. V. Shokurov, 1995: Patterns of interannual variability defined by a cluster analysis and their relation with enso. *Quarterly Journal of the Royal Meteorological Society*, **121**, 1651–1679.
- Franzke, C., D. Crommelin, A. Fischer, and A. Majda, 2007: A hidden markov model perspective on regimes and metastability in atmospheric flows. *J. Climate*, (**submitted**) (**22**).
- Gardiner, H., 2004: *Handbook of stochastic methods*. Springer, Berlin.
- Horenko, I., R. Klein, S. Dolaptchiev, and C. Schuette, 2008: Automated generation of reduced stochastic weather models i: simultaneous dimension and model reduction for time series analysis. *SIAM MMS*, **6(4)**.
- Horenko, I., J. Schmidt-Ehrenberg, and C. Schütte, 2006: Set-oriented dimension reduction: Localizing Principal Component Analysis via Hidden Markov Models. *CompLife 2006*, R. G. M.R. Berthold and I. Fischer, Eds., Springer, Berlin Heidelberg, Lecture Notes in Bioinformatics, Vol. 4216, 98–115.
- Horenko, I. and C. Schuette, 2007: Dimension reduction for time series with hidden phase transitions and economic applications. *submitted to the Econometrics Journal*, (available via [biocomputing.mi.fu-berlin.de](http://biocomputing.mi.fu-berlin.de)).

- Kimoto, M. and M. Ghil, 1993a: Multiple flow regimes in the northern hemisphere winter. part i: Methodology and hemispheric regimes. *Journal of Atmospheric Sciences*, **50**, 2625–2644.
- Kimoto, M. and M. Ghil, 1993b: Multiple flow regimes in the northern hemisphere winter. part ii: Sectorial regimes and preferred transitions. *Journal of Atmospheric Sciences*, **50**, 2645–2673.
- Lupo, A. R., R. J. Oglesby, and I. I. Mokhov, 1997: Climatological features of blocking anticyclones: a study of northern hemisphere ccm1 model blocking events in present-day and double co<sub>2</sub> concentration atmospheres. *Climate Dynamics*, **13**, 181–195.
- Majda, A., C. Franzke, A. Fischer, and D. Crommelin, 2006: Distinct metastable atmospheric regimes despite nearly gaussian statistics : A paradigm model. *PNAS*, **103 (22)**, 8309–8314.
- Mardia, K., J. Kent, and J. Bibby, 1979: *Multivariate Analysis*. Academic Press.
- Mokhov, I., V. Petukhov, and V. Semenov, 1998: Multiple intraseasonal temperature regimes and their evolution in the iap ras climate model. *Izvestiya, Atmos. Ocean. Phys.*, **34**, 145–152.
- Mokhov, I. and V. Semenov, 1997: Bimodality of the probability density functions of subseasonal variations in surface air temperature. *Izvestiya, Atmos. Ocean. Phys.*, **33**, 702–708.
- Nicolis, C., 1982: Stochastic aspects of climatic transitions-response to a periodic forcing. *Tellus*, **34**, 1–+.

- Paillard, D., 1998: The timing of pleistocene glaciations from a simple multiple-state climate model. *Nature*, **391**, 378–381, doi:10.1038/34891.
- Palmer, T. N., 1999: A Nonlinear Dynamical Perspective on Climate Prediction. *Journal of Climate*, **12**, 575–591.
- Rex, D. F., 1950a: Blocking action in the middle troposphere and its effects upon regional climate. i: An aerological study of blocking action. *Tellus*, **2**, 196–211.
- Rex, D. F., 1950b: Blocking action in the middle troposphere and its effects upon regional climate. ii: The climatology of blocking action. *Tellus*, **2**, 275–301.
- Schütte, C. and W. Huisinga, 2003: Biomolecular conformations can be identified as metastable sets of molecular dynamics. *Handbook of Numerical Analysis*, P. G. Ciaret and J.-L. Lions, Eds., Elsevier, Vol. X, 699–744.
- Simmons, A. and J. Gibson, 2000: The ERA 40 project plan. *ERA 40 Project Rep. Ser. 1*, european Center for Medium-Range Weather Forecasting, Reading.
- Strang, G. and T. Nguyen, 1997: *Wavelets and Filter Banks*. Wellesley-Cambridge Press, Wellesley.
- Tsay, R., 2005: *Analysis of financial time series*. Wiley Series in Probability and Statistics.
- Tsonis, A. and J. Elsner, 1990: Multiple attractors, fractal basins and longterm climate dynamics. *Beit. Phys. Atmos.*, **63**, 171–176.
- Viterbi, A., 1967: Error bounds for convolutional codes and an asymptotically optimum decoding algorithm. *IEEE Trans. Informat. Theory*, **13**, 260–269.

Wiedenmann, J. M., A. R. Lupo, I. I. Mokhov, and E. A. Tikhonova, 2002: The climatology of blocking anticyclones for the northern and southern hemispheres: Block intensity as a diagnostic. *Journal of Climate*, **15**, 3459–3473.

# List of Figures

1	Left: dominant eigenvalues of the autocorrelation matrix (left) and of the AR-coefficients (right), computed for different time lags. . . . .	40
2	Spectrum of the hidden transition matrix $A$ for $K = 8$ . Only first 4 dominant eigenvalues are statistically significant since the parameter confidence intervals of the hidden states correspondent to the lower part of the spectrum (eigenvalues 5 – 8) are overlapping. This indicates $K=4$ as the upper bound for the number of statistically distinguishable hidden states. . . . .	41
3	Comparison of hidden Viterbi-paths identified with Wavelets-PCA (dashed) and HMM-PCA (solid) algorithms (both for $K = 4, d = 5$ ). . . . .	42
4	The Viterbi path of the hidden Markov chain for different resolutions of the data and different frame lengths $d$ : results from data on a $32 \times 18$ grid (lines), on a $16 \times 9$ grid (dots dashes, only for $d = 1, 5$ ). . . . .	43
5	The vector $\mu_i$ for the four different hidden states computed using a frame length of 1 day and data on the $31 \times 18$ grid. . . . .	44
6	The same as in Fig.5 but on the $16 \times 9$ grid. . . . .	45
7	The computed onset composite $x^o(q)$ at different time lags $q$ . For $x_{t_j}$ in (32) we have used data with annual cycle, units are gpdm. . . . .	46
8	The computed withdraw composite $x^w(q)$ at different time lags $q$ . For $x_{t_j}$ in (33) we have used data with annual cycle, units are gpdm. . . . .	47
9	The time evolution of the zonally averaged blocking index (dashes) and the probability for hidden state four $\gamma_4$ (solid line). . . . .	48

10	The vector $\mu_4$ at different time lags $t$ computed using a frame length of 5 and the $31 \times 18$ resolution. . . . .	49
11	Zonally averaged geopotential height difference between $40^\circ$ N and $60^\circ$ N for the $\mu_i$ vectors at different time lags. The plots represent the results for different frame lengths $d$ . The values for $d = 1$ are indicated by lines with markers in the first plot, where squares, stars, circles and diamonds correspond to state 3, 1, 2 and 4, respectively. . . . .	50
12	Graphic representation of the hidden Markov process responsible for the metastable behavior of the analyzed time series (identified with HMM-PCA-algorithm for $K = 4, m = 1, d = 5$ ). Circles denote the hidden states and arrows show the connections between them, the numbers represent respective probabilities of transitions. . . . .	51



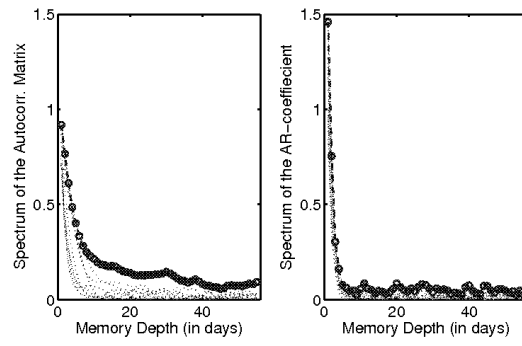


FIG. 1. Left: dominant eigenvalues of the autocorrelation matrix (left) and of the AR-coefficients (right), computed for different time lags.

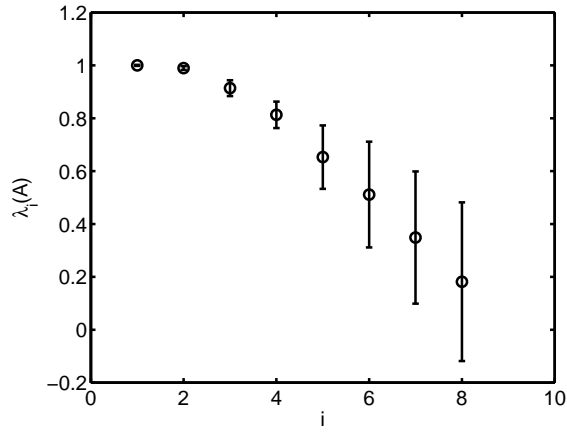


FIG. 2. Spectrum of the hidden transition matrix  $A$  for  $K = 8$ . Only first 4 dominant eigenvalues are statistically significant since the parameter confidence intervals of the hidden states correspondent to the lower part of the spectrum (eigenvalues 5 – 8) are overlapping. This indicates  $K=4$  as the upper bound for the number of statistically distinguishable hidden states.

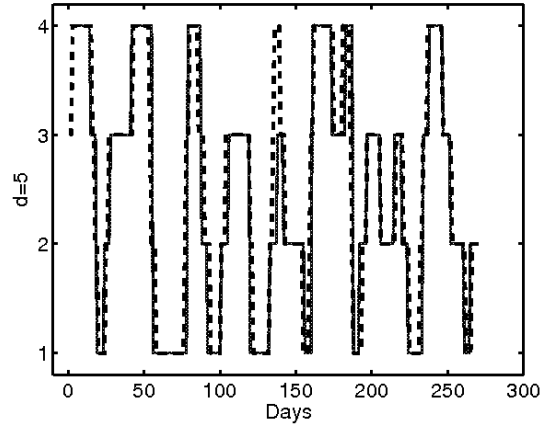


FIG. 3. Comparison of hidden Viterbi-paths identified with Wavelets-PCA (dashed) and HMM-PCA (solid) algorithms (both for  $K = 4, d = 5$ ).

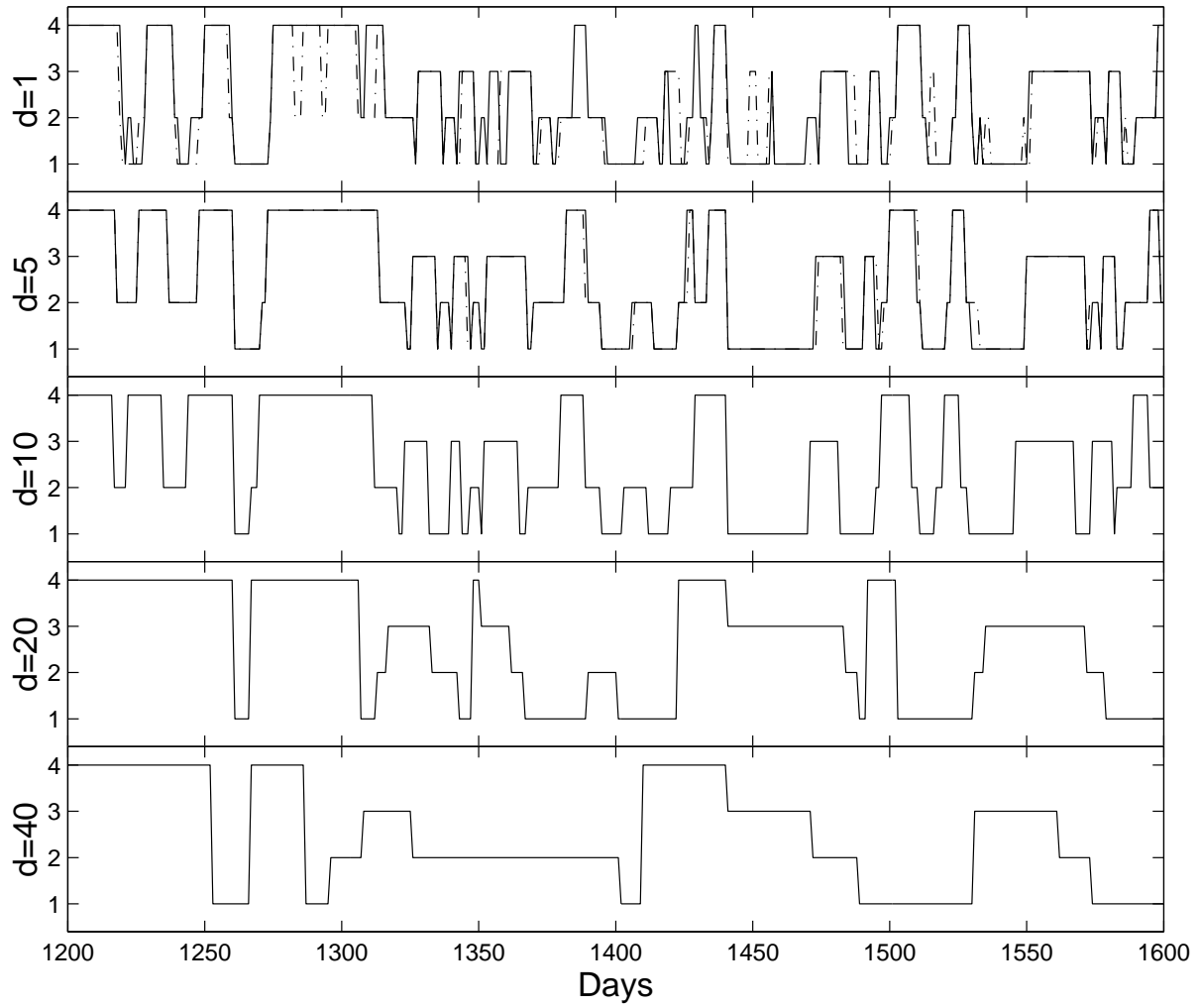


FIG. 4. The Viterbi path of the hidden Markov chain for different resolutions of the data and different frame lengths  $d$ : results from data on a  $32 \times 18$  grid (lines), on a  $16 \times 9$  grid (dots dashes, only for  $d = 1, 5$ ).

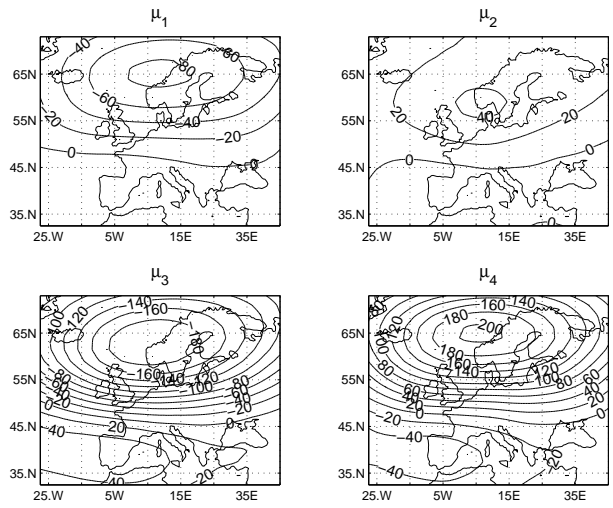


FIG. 5. The vector  $\mu_i$  for the four different hidden states computed using a frame length of 1 day and data on the  $31 \times 18$  grid.

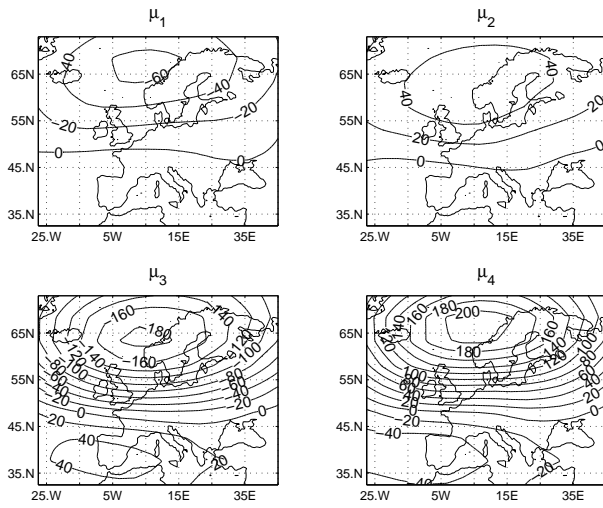


FIG. 6. The same as in Fig.5 but on the  $16 \times 9$  grid.

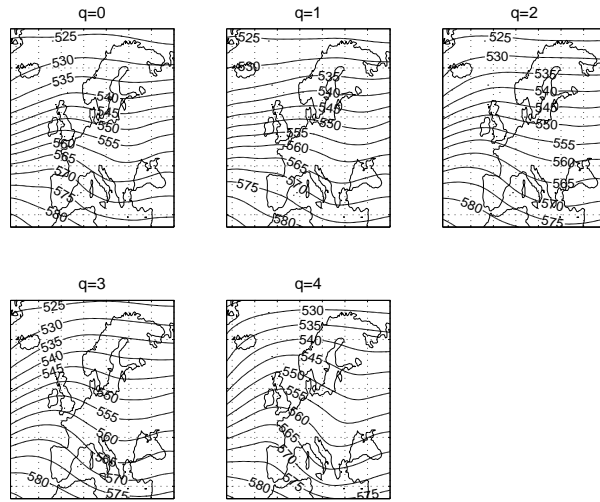


FIG. 7. The computed onset composite  $x^o(q)$  at different time lags  $q$ . For  $x_{t_j}$  in (32) we have used data with annual cycle, units are gpd/m.

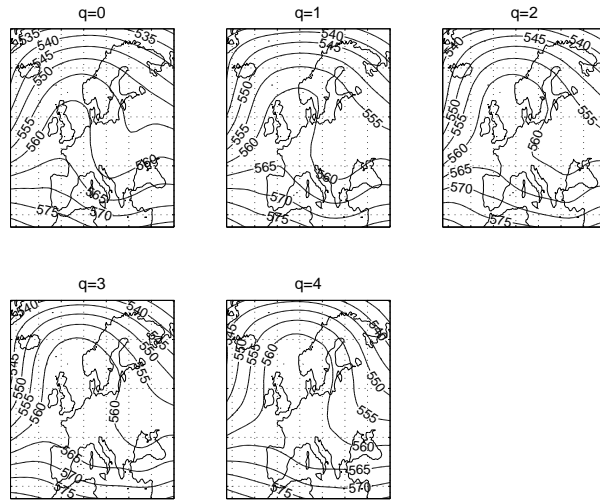


FIG. 8. The computed withdraw composite  $x^w(q)$  at different time lags  $q$ . For  $x_{t_j}$  in (33) we have used data with anual cycle, units are gpdm.



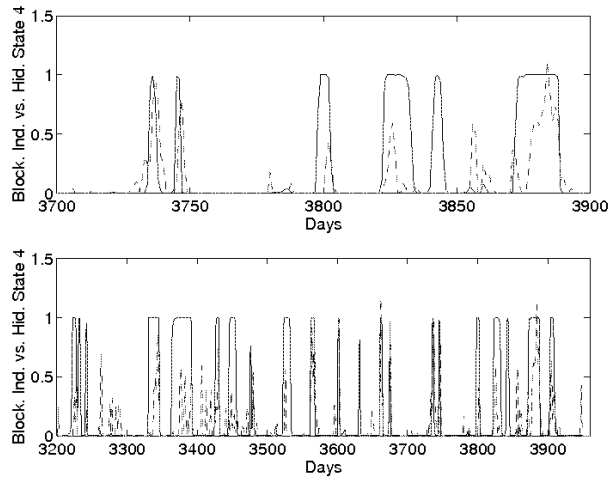


FIG. 9. The time evolution of the zonally averaged blocking index (dashes) and the probability for hidden state four  $\gamma_4$  (solid line).

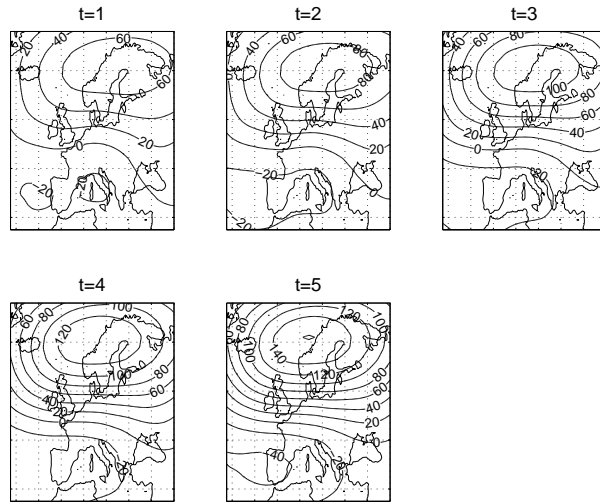


FIG. 10. The vector  $\mu_4$  at different time lags  $t$  computed using a frame length of 5 and the  $31 \times 18$  resolution.

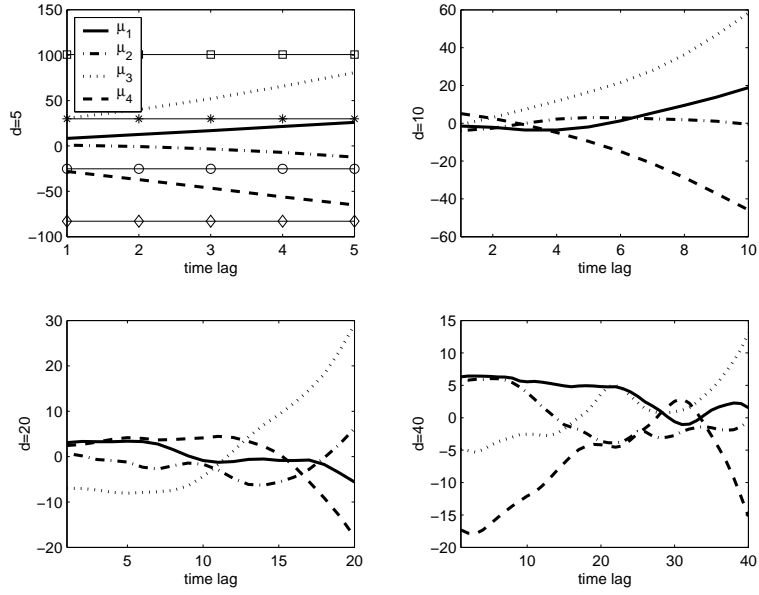


FIG. 11. Zonally averaged geopotential height difference between 40° N and 60° N for the  $\mu_i$  vectors at different time lags. The plots represent the results for different frame lengths  $d$ . The values for  $d = 1$  are indicated by lines with markers in the first plot, where squares, stars, circles and diamonds correspond to state 3, 1, 2 and 4, respectively.

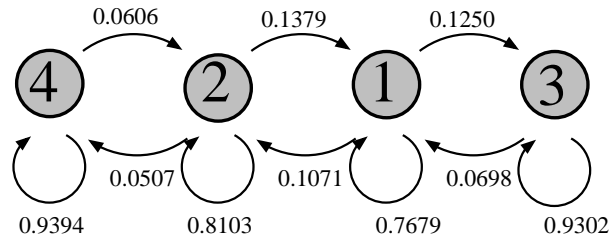


FIG. 12. Graphic representation of the hidden Markov process responsible for the metastable behavior of the analyzed time series (identified with HMM-PCA-algorithm for  $K = 4, m = 1, d = 5$ ). Circles denote the hidden states and arrows show the connections between them, the numbers represent respective probabilities of transitions.